LA-UR-15-26063 (Accepted Manuscript)

Examination of the - two-phase shock-induced microstructure in zirconium and titanium

Morrow, Benjamin
Escobedo, J. Pablo
Field, Robert Douglas
Dickerson, Robert Michael
Dickerson, Patricia O'Donnell
Trujillo, Carl Patrick
Cerreta, Ellen Kathleen

To be published in:

DOI to publisher's version: 10.1063/1.4971658

Permalink to record: http://permalink.lanl.gov/object/view?what=info:lanl-repo/lareport/LA-UR-15-26063

Examination of the α-ω Two-Phase Shock-Induced Microstructure in Zirconium and Titanium

Benjamin M. Morrow[*], J. Pablo Escobedo[†], Robert D. Field[*,**], Robert M. Dickerson[*], Patricia O. Dickerson[*], Carl P. Trujillo[*] and Ellen K. Cerreta[*]

[*]*Los Alamos National Laboratory, P.O. Box 1663, MS G755, Los Alamos, NM 87545, USA*
[†]*University of New South Wales, Australia*
[**]*Colorado School of Mines, USA*

Abstract.
Omega (ω) phase is formed in alpha (α) zirconium during dynamic loading and can be retained in the recovered material. The pathway for the α to ω change (or the reverse transformation) is not well understood. Zirconium was shock-loaded and the resulting two-phase microstructure was examined. Electron backscatter diffraction (EBSD) was used to characterize the orientation relationships and habit planes between phases to understand the pathways between α and ω phases and compare to Molecular Dynamics (MD) simulations. Based on key microstructural features, a significant amount of α phase appears to have originated from the reverse transformation from ω-Zr on unloading. Results of microstructural analysis will be discussed, along with implications toward phase transformation pathways.

Keywords: Shock; Dynamic Compression; Phase Transformation; Zirconium
PACS: 64.70.K-; 68.37.Hk; 83.50.-v;

INTRODUCTION

The mechanical response of hexagonal close-packed (hcp) materials in complex loading environments experienced in automotive, aerospace, nuclear energy and biomedical applications is extremely important [1]. The evolution of microstructure is of particular importance to understanding mechanical behavior and failure in hcp metals. Traditional plasticity mechanisms have been studied in the past over a range of length and time scales [2–7], and are reasonably well-understood. However, both zirconium and titanium undergo a solid state phase transformation under dynamic conditions wherein the material changes from hcp α phase to hexagonal ω phase [8, 9]. The observed mechanical behavior is then influenced by the coupled evolution of plastic and phase transformation processes.

Zirconium (used in this work) is a model system to study the phase transition in hcp metals. Previous work by Cerreta et al. showed that ω phase begins to form above 7 GPa under dynamic conditions [10]. Additionally, Cerreta showed that by increasing the dynamic drive condition (a function of test velocity or peak stress and temperature) the amount of retained ω phase also increases. Retained ω was also shown to influence subsequent mechanical behavior during quasi-static loading. Specifically, yield strength increased and work hardening rate decreased with increasing retained ω phase. This behavior underscores the importance of the α-ω phase transformation to mechanical properties. Because of this, the crystallography of the phase transition will be studied, to gain insight into nucleation of ω phase and the transformation mechanisms and pathways, which are important to support subsequent modeling efforts.

EXPERIMENTAL METHODS

High-purity, crystal bar Zr was used in this work. The material was a highly textured polycrystal, with the c-axes of nearly all grains aligned in the loading direction. The specimen examined in the current work was dynamically loaded parallel to the strongly textured direction using plate impact with a Zr impactor. Flyer velocity was 658 m/s, corresponding to a peak stress of $\sim$8.5 GPa. Testing was performed at room temperature. The specimen was soft-recovered after loading, then sectioned and prepared using standard metallographic techniques for microstructural characterization. Previous work showed that the microstructure contains $\sim$65% retained ω phase at these conditions [10].

An FEI Inspect scanning electron microscope (SEM) equipped with an EDAX electron backscatter diffraction (EBSD) system was used to collect phase and orientation information. Orientation relationships between adjacent α

and ω regions were calculated from this orientation data. To obtain the habit plane for the α-ω interface, a two-surface technique was used, similar to that proposed by Cahn [11]. An FEI Helios dual-beam focused ion beam (FIB) was used to prepare a foil from the volume beneath the surface for analysis in both the transmission electron microscope (TEM) and SEM. This was done to obtain orientation of each phase and the plane trace for a single α-ω boundary from multiple viewing directions, enabling the habit plane to be determined through standard stereographic analysis. Figure 1 shows inverse pole figure (IPF) plots for each surface used in the analysis. In the figure, the subsurface foil data has been rotated to align with the orientations of original surface to allow for easy identification of corresponding α and ω regions. Raw, unrotated data was used for the stereographic analysis. An FEI Tecnai TEM was used to perform tilting experiments to measure orientation relationships (OR) and habit plane and compare to EBSD analysis.

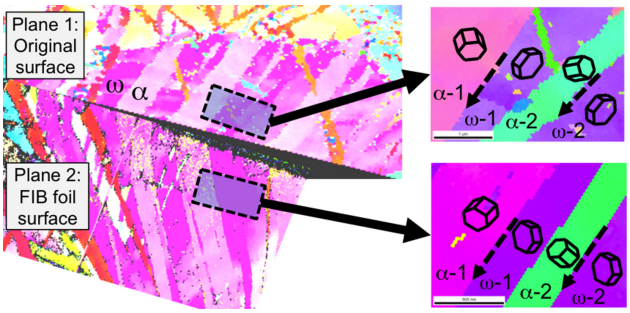

FIGURE 1. IPFs from EBSD showing original and subsurface foil surfaces in shocked zirconium specimen. Insets show detail of multiple adjacent α-ω boundaries.

RESULTS AND DISCUSSION

Orientation information obtained from EBSD was used to determine orientation relationships between phases, as well as habit plane for an α-ω boundary. A review of the EBSD technique and its application to phase identification and orientation measurement can be found elsewhere [12]. For the purposes of this study, all measurements originated from multiple phase fragments (distinct regions) within a single grain of a shocked Zr specimen. Lattice parameters used were: a_α=3.232 Å, c_α=5.147 Å, a_ω=5.039 Å, c_ω=3.136 Å for Zr [8]; and a_α=2.95 Å, c_α=4.68 Å, a_ω=4.621 Å, c_ω=2.817 Å for Ti [8]. The grain, shown in Figure 1, shows parallel laths of α and ω phase, as well as a few, smaller additional variants of α contained by ω regions. Several different values for the α-ω phase boundary have been observed in Zr previously [8–10, 13, 14]. Through direct comparison of orientation information from each phase across several boundaries, it was determined that the orientation relationship satisfied for all laths in the grain of interest was $\{0001\}_\alpha \| \{10\bar{1}1\}_\omega$, $\langle 10\bar{1}0\rangle_\alpha \| \langle \bar{1}\bar{1}23\rangle_\omega$. This relationship was confirmed by TEM analysis, and is consistent with literature [9]. EBSD poses an advantage over traditional methods of OR measurement, as it allows for much more rapid collection of orientation data. This can be used to rapidly assess orientation relationships in two-phase hcp metals across many boundaries and grains, and facilitates the collection of detailed statistics for phase transformations, similar to previous work on twinning in Zr [15].

While the trace of an α-ω boundary plane can be determined from any two-dimensional section (i.e. an EBSD scan or TEM micrograph), two separate viewing directions are needed to determine the habit plane. Figure 1 shows orientation information and plane traces from two orthogonal directions. By measuring each plane trace and comparing them stereographically, the habit plane of an α-ω boundary was determined by the cross product of the two projections. The habit plane between α_1 and ω_1 laths shown in Figure 1 was $\left(\bar{1}\bar{3}40\right)_{\alpha_1} \| \left(\overline{10}\ \bar{1}\ 11\ \bar{1}\right)_{\omega_1}$. TEM analysis was used to obtain supplemental orientation information to confirm the EBSD results. Boundaries are not always completely planar or regular, contributing error to the stereographic analysis. As a result, the habit plane may vary slightly from this analysis. Future analysis will provide information for other α-ω boundaries and build a statistical representation of measurements.

The relationships between phases present can be determined through examination of individual boundaries, as above. However, the pathways for transformation between phases is not captured in a single boundary, and lie instead at the grain level. For this, we turn to EBSD of entire grains, including all grain fragments of different phases within. The zirconium studied in this work was a highly textured polycrystal, so to determine the deformation behavior

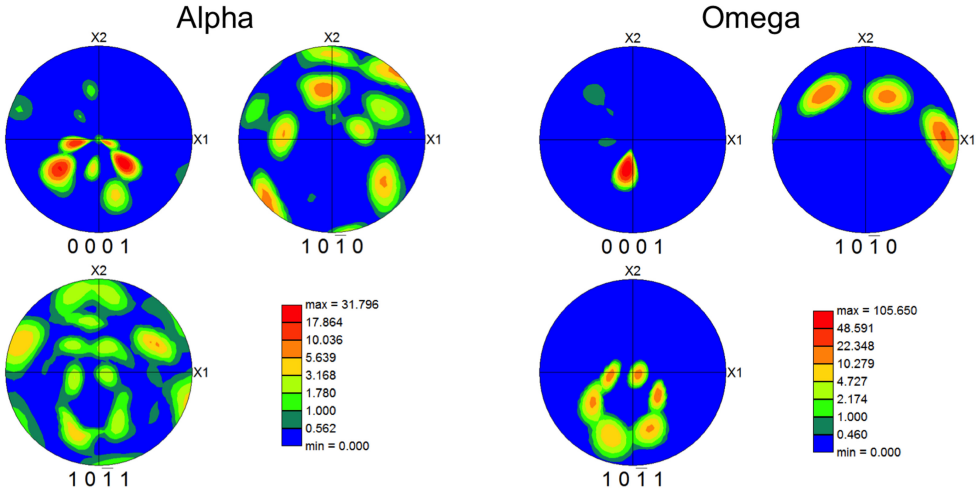

FIGURE 2. Pole figures showing textures for α and ω phase zirconium loaded using plate impact shock.

through post-mortem texture a single grain was chosen, analyzing all fragments within the grain. Figure 2 shows the microtexture pole figures for α and ω-Zr, loaded by plate impact to a peak stress of 8 GPa. A single strong peak appears in the center of the $(0001)_\omega$ pole figure, indicating a single parent orientation shared by all of the ω phase fragments. Several strong peaks at different orientations in the $(0001)_\alpha$ pole figure in Figure 2 are also visible, corresponding to several different variants of α phase within the region of interest. Crystallographically, it is expected that each grain starts with a single parent orientation. As new phases form within the parent, they adopt one of several possible crystallographic variants, resulting in multiple peaks of different orientation corresponding to the newly formed daughter phase. In this case, the single ω peak is likely the original parent, while each of the several strong α peaks is a daughter phase formed from the original ω parent. Based on this analysis, it is likely that the zirconium displays a reverse ($\omega \rightarrow \alpha$) phase transition under these test conditions. A similar phase change, as a result of heating instead of accumulated strain, has been observed previously [16]. Because the Zr specimen was entirely α phase prior to dynamic loading, the original $\alpha \rightarrow \omega$ phase transformation was not captured in the post-mortem microstructure.

For comparison, the EBSD microtexture of a single crystal specimen of titanium from previous work, loaded by plate impact to a peak stress of 13.5 GPa is presented in Figure 3. The $(0001)_\alpha$ pole figure in Figure 3 shows one strong peak in the center corresponding to a single orientation shared by most of the α phase grain fragments. Less intense peaks around the center represent the six unique compression twin variants expected for this orientation. Figure 3 also shows the texture for the ω phase grain fragments of the single grain. In contrast to the α phase, several variants of ω, represented by six strong peaks arranged around the center of the $(0001)_\omega$ pole figure, can be seen in Figure 3. By applying the same parent-daughter analysis as before, the dynamically loaded Ti shown in Figure 3 likely displays the forward, $\alpha \rightarrow \omega$ phase transition.

The different textures indicate two separate pathways for the α-ω phase transformation in Zr and Ti, yielding two distinctly different microstructural endpoints. Each parent (ω in Zr and α in Ti) had a single initial orientation, and produced multiple orientation variants of the daughter phase. It is reasonable to suggest that variant selection for phase transformation will have a large impact on resulting microstructure and, as a result, the subsequent mechanical properties. Additionally, evidence of twinning in the α phase (see Figure 3) suggests that the observed dynamic mechanical behavior is a layered effect of traditional plasticity as well as the α-ω phase change(s). The role of twinning, if any, in the forward transformation is not well understood at present.

CONCLUSION

Zirconium was dynamically loaded with plate impact shock experiments. Samples were soft-recovered for post-mortem analysis. A two-phase microstructure was present, consisting of the original hcp α phase and newly formed hexagonal ω phase. EBSD was used to measure orientation information from each phase. The orientation relationships,

determined through EBSD and confirmed by TEM, are in agreement with previously established literature values. The habit plane was determined through EBSD and confirmed with TEM. Microtextures for Zr and Ti reveal two distinctly different pathways for the solid-solid phase transformation: the forward, $\alpha \rightarrow \omega$ transition (for Ti) and the reverse, $\omega \rightarrow \alpha$ transition (for Zr). The orientation relationships appear similar for each pathway, but the mechanisms for the transformation may be different, especially given differing endpoint microstructures.

ACKNOWLEDGMENTS

The authors would like to thank Dr. Rodney J. McCabe for helpful discussions. Los Alamos National Laboratory is operated by LANS, LLC, for the NNSA of the US Department of Energy under contract DE-AC52-06NA25396. The LDRD and Campaign 2 programs supported this work. LA-UR-15-26063.

REFERENCES

1. B. M. Morrow, S. N. Mathaudhu, E. K. Cerreta, J. P. Escobedo-Diaz, and D. R. Trinkle, *Metallurgical and Materials Transactions A* **45**, 5876 (2014).
2. E. Cerreta, and G. T. Gray, III, *Metallurgical and Materials Transactions A* **35**, 1999–2011 (2004).
3. E. Cerreta, C. A. Yablinsky, G. T. Gray, III, S. C. Vogel, and D. W. Brown, *Materials Science and Engineering A* **456**, 243–251 (2007).
4. B. M. Morrow, R. W. Kozar, K. R. Anderson, and M. J. Mills, *Acta Materialia* **61**, 4452–4460 (2013).
5. B. M. Morrow, R. J. McCabe, E. K. Cerreta, and C. N. Tomé, *Metallurgical and Materials Transactions A* **45**, 36–40 (2014).
6. B. M. Morrow, R. J. McCabe, E. K. Cerreta, and C. N. Tomé, *Metallurgical and Materials Transactions A* **45**, 5891–5897 (2014).
7. B. M. Morrow, E. K. Cerreta, R. J. McCabe, and C. N. Tomé, *JOM* **67**, 1721–1728 (2015).
8. S. K. Sikka, Y. K. Vohra, and R. Chidambaram, *Progress in Materials Science* **27**, 245–310 (1982).
9. S. G. Song, and G. T. Gray, III, *Philosophical Magazine A* **71**, 275–290 (1995).
10. E. K. Cerreta, J. P. Escobedo, P. A. Rigg, C. P. Trujillo, D. W. Brown, T. A. Sisneros, B. Clausen, M. F. Lopez, T. Lookman, C. A. Bronkhorst, and F. L. Addessio, *Acta Materialia* **61**, 7712–7719 (2013).
11. R. W. Cahn, *Acta Metallurgica* **1**, 49–70 (1953).
12. F. J. Humphreys, *Journal of Materials Science* **36**, 3833–3854 (2001).
13. M. P. Usikov, and V. A. Zilbershtein, *Physica Status Solidi A* **19**, 53–58 (1973).
14. A. Rabinkin, M. Talianker, and O. Botstein, *Acta Metallurgica* **29**, 691–698 (1981).
15. B. M. Morrow, R. J. McCabe, E. K. Cerreta, and C. N. Tomé, *Materials Science and Engineering: A* **574**, 157–162 (2013).
16. D. W. Brown, J. D. Almer, L. Balogh, E. K. Cerreta, B. Clausen, J. P. Escobedo-Diaz, T. A. Sisneros, P. L. Mosbrucker, E. F. Tulk, and S. C. Vogel, *Acta Materialia* **67**, 383–394 (2014).

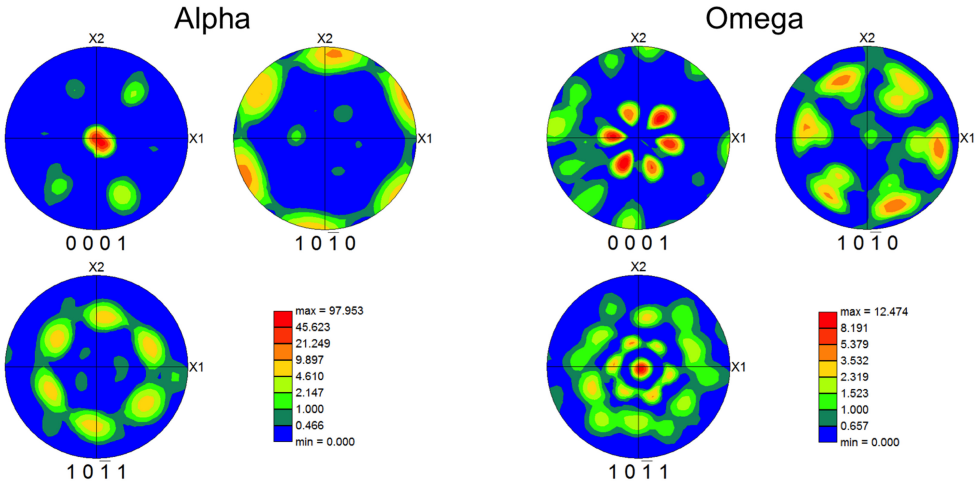

FIGURE 3. Pole figures showing textures for α and ω phase titanium loaded using plate impact shock.